Algal Research 72 (2023) 103082

Contents lists available at ScienceDirect

Algal Research

journal homepage: www.elsevier.com/locate/algal

Light absorption by *Volvocaceae* colonies consisting of equidistant optically soft photosynthetic cells in a transparent spherical extracellular matrix

Jack Hoeniges [a], Arka Bhowmik [b], Refet A. Yalçin [a], Vincent J. Partusch [a], Laurent Pilon [a,*]

[a] *Mechanical and Aerospace Engineering Department, Henry Samueli School of Engineering and Applied Science, University of California, 420 Westwood Plaza, Los Angeles, CA 90095, USA*
[b] *Department of Radiology, Memorial Sloan Kettering Cancer Center, 1275 York venue, New York, NY 10065, USA*

ARTICLE INFO

Keywords:
Light transfer
Optical properties
Absorption
T-matrix
Ray tracing

ABSTRACT

This study aims to develop a methodology to predict the absorption cross-section of colonial microalgae such as those of the *Volvocaceae* family including *Eudorina*, *Pleodorina*, and *Volvox* consisting of an ordered assembly of large and optically soft absorbing cells embedded within a non-absorbing spherical extracellular matrix (ECM). The absorption cross-section of spherical colonies, such as *Eudorina*, containing 16, 32, and 64 equidistant photosynthetic cells distributed on the surface of a sphere within a concentric spherical ECM was predicted by the superposition T-matrix method for ECM size parameters as large as 500 and by the Monte Carlo ray-tracing (MCRT) method for ECM size parameters as large as 900. The predicted absorption cross-sections given by the two methods were in excellent agreement despite the fact that the conditions for geometric optics were not rigorously satisfied. The absorption cross-section of the microalgae colonies considered was found to increase with increasing cell radius, absorption index or cell pigment concentration, and/or number of cells. Shading among cells decreased the mass absorption cross-section and was increasingly important for colonies with strongly absorbing cells, large cell radius, and/or large number of cells. These results demonstrate that accounting for shading effects is necessary to accurately predict the absorption cross-section of microalgae colonies. Furthermore, the study demonstrated that the MCRT method is an accurate and efficient method for modeling light absorption by an ensemble of many large, ordered, and optically soft particles. Finally, the impact of colony formation as well as pigment and biomass concentrations on the local (LRPA) and mean (MRPA) rates of photon absorption within a microalgae culture was also assessed. At low biomass concentrations, the LRPA and MRPA decreased in the presence of colonies. This effect was more pronounced at higher pigment concentrations.

1. Introduction

Photosynthetic microorganisms or microalgae are found in diverse forms including unicellular and multicellular organisms as well as colonies. For example, colonial green microalgae *Eudorina*, *Pleodorina*, and *Volvox* in the *Volvocaceae* family, consist of an ensemble of independent and nearly equidistant unicellular photosynthetic cells embedded in an extracellular matrix (ECM) made of glycoprotein [1]. The cells are considered close relatives of the unicellular green microalgae *Chlamydomonas* [2]. In these colonial microalgae, cell division no longer results in unicellular individuals but instead leads to so-called autocolonies [1,3,4]. Fig. 1 shows micrographs of (a) free floating *Chlamydomonas reinhardtii*, (b) *Eudorina elegans*, (c) *Pleodorina californica*, and (d) *Volvox aureus*.

Microalgae colonies such as *Eudorina*, *Pleodorina*, and *Volvox* have been studied extensively due to their negative impact on aquatic ecosystems [5–9] and on water treatment plants [10,11]. Indeed, their ability to reproduce rapidly in nutrient-rich water often leads to the formation of scum on the water surface [5]. This excessive growth may (a) change the taste and odor of public water supplies [10,11], (b) interfere with the filtration process of water treatment plants [10], and (c) threaten the survival of other aquatic species by depleting their nutrient and oxygen supplies [6,8]. These issues have drawn significant interest among limnologists, environmental agencies, water authorities, and human/animal health organizations to effectively monitor phytoplankton blooms in rivers, lakes, ponds, and coastal and open oceans using satellite remote sensing [12,13]. In fact, remote sensing techniques are widely used to detect, identify, and monitor harmful algal

* Corresponding author.
E-mail address: pilon@seas.ucla.edu (L. Pilon).

https://doi.org/10.1016/j.algal.2023.103082
Received 22 April 2022; Received in revised form 20 February 2023; Accepted 31 March 2023
Available online 14 April 2023

blooms by monitoring spatiotemporal changes in Chlorophyll *a* (Chl. *a*) concentration maps obtained using multispectral imaging [12,13]. To do so, Chl. *a* concentration maps are produced by fitting the measured spectral reflectance with a theoretical model based on some solution of the radiative transfer equation using the radiation characteristics of microalgae and colonies and in particular their absorption cross-section [14–16].

Moreover, colony-forming microalgae species have been used in a wide range of biotechnological applications. For instance, microbial proteins derived from *Volvox carteri* which respond to photostimulation by yellow light have been studied for potential application in optogenetics [17]. Furthermore, flocculation in non-colony forming microalgae such as *Chlamydomonas reinhardtii* can be induced by heterologous expression of a cell adhesion molecule also found in *Volvox carteri* [18]. Additionally, *Eudorina elegans* has been studied for its potential use in phycoremediation. Indeed, the high levels of surface mucilage present on the surface of the ECM of *Eudorina elegans* enable superior absorption of heavy metals such as copper compared to single cell species such as *Chlorella vulgaris* [19]. *Eudorina elegans* has also been used as part of a biosensor featuring a consortium of microalgae strains immobilized on a permeable membrane for real-time monitoring of water-soluble herbicides [20].

For all such applications, efficient cultivation of colony-forming microalgae is essential. Cultivation typically occurs in photobioreactors (PBRs) where operational parameters such as temperature, pH, and nutrient availability can be controlled. Maximum PBR productivity occurs in the light-limited regime, wherein these parameters are maintained at their optimum and culture growth depends only on the quantity of photons absorbed by the cells [21]. The latter is represented by the local rate of photon absorption (LRPA) in $\mu mol_{h\nu} g^{-1} s^{-1}$ at a given culture depth [21]. The LRPA depends on a variety of operational and design factors such as the PBR geometry, culture depth, cell concentration, and incident photosynthetic photon flux as well as the radiative properties of the microalgae species being cultivated, i.e., their scattering and absorption cross-sections and scattering phase function [22]. However, microalgae cells tend to be strongly forward scattering due to their relatively large size compared to the wavelength of light in the photosynthetically active radiation (PAR) region. Thus, previous studies have demonstrated that the LRPA can be accurately estimated using only the absorption cross-section [22,23]. Thus, predicting the absorption cross-section of microalgae cells and colonies is sufficient for predicting, optimizing, and controlling the biomass growth in PBRs.

The absorption cross-section of microalgae in suspension has been determined either experimentally [16,22,24–28] or numerically [16,29–35]. Experimental methods can account for the actual shape and size distribution of microalgae in suspension. For example, Kandilian et al. [22] used an inverse method to retrieve the average spectral absorption cross-section of microalgae from measurements of the normal-hemispherical transmittance and reflectance of a cuvette containing a polydisperse suspension of quasi-spherical microalgae. However, a microalgae suspension will contain colonies of varying maturity featuring different numbers of cells per colony and colony and cell radius, making it difficult to isolate the influence these parameters on the colony absorption cross-section. Furthermore, such methods are only valid for specific growth conditions and can be time-consuming and expensive as they require sophisticated equipment [36].

Numerical studies predicting the radiation characteristics of particle aggregates have used the superposition T-matrix method [37], the Monte Carlo ray-tracing (MCRT) method [35,38,39], the generalized multi-particle Mie method [40], the volume integral method [41], or the hybrid finite element-boundary integral method [42]. Specifically, the superposition T-matrix method has been used to predict the radiation characteristics of multicellular cyanobacteria [32,33] and fractal microalgae colonies [34]. However, this method can be prohibitively resource-intensive when the number of particles and/or their size is large. Thus, these studies only considered cells with relatively small size parameters x of less than 20. Here x is defined as $x = 2\pi r/\lambda$ with r being the radius of the particle (e.g., the microalgae cells) and λ being the free space wavelength of the incident radiation. However, a colony of *Eudorina elegans*, for example, consists of 16, 32, or 64, equidistant reproductive cells, 5–10 μm in radius, embedded in an ECM with radius ranging from 45 to 75 μm depending on the maturity of the colony [4,43–45]. Then, the size parameters corresponding to the cell and ECM radii can range from approximately 40 to 90 and 400 to 1200, respectively, over the PAR region from 400 to 750 nm.

Our previous study [35] compared the average absorption cross-sections of suspensions of free-floating single cells or fractal colonies of *Botryococcus braunii* cells measured experimentally and predicted by

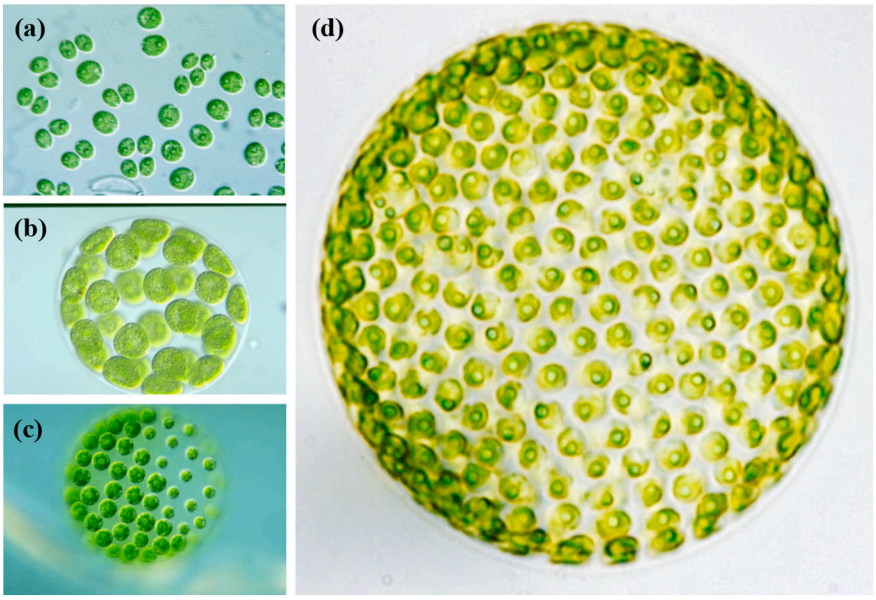

Fig. 1. Micrographs of members of the *Volvocaceae* family and its close relatives: (a) free floating *Chlamydomonas reinhardtii*†, (b) *Eudorina elegans*†, (c) *Pleodorina californica*†, and (d) *Volvox aureus*. †Reproduced with permission from Prof. Yuuji Tsukii (Hosei University, http://protist.i.hosei.ac.jp/). The micrograph of *Volvox aureus* was imaged in our laboratory.

the MCRT method. Colonies were modeled as fractal aggregates of spherical cells of radius $r_c = 3.71$ μm. Colonies embedded in a non-absorbing spherical ECM with radius r_{ECM} were also considered. The MCRT method was shown to accurately model absorption by fractal colonies with cell size parameter $x = 10$ and up to 25 constituent cells and cell size parameter $x = 20$ and up to 16 constituent cells by comparing its predictions with those from the T-matrix method. Note also that the scattering cross-section of fractal colonies of optically soft cells could not be predicted using the MCRT method [35]. Indeed, large optically soft particles, such as microalgae cells and colonies, fall under the anomalous diffraction scattering regime wherein the scattering efficiency factor Q_{sca} remains dependent on diffraction and interference effects [46,47]. However, these phenomena cannot be captured by the MCRT method since it neglects wave effects. Overall, the experimental measurements showed that the mass absorption cross-section (in m^2kg^{-1}) of *B. braunii* was much smaller for a culture containing colonies than for one containing only single cells. Part of this decrease was attributed to the lower pigment concentration in the culture with colonies present. However, for a given pigment concentration, the MCRT also predicted a decrease in the average mass absorption cross-section of colonies with increasing number of cells N_c due to mutual shading among cells. To assess the impact of cell arrangement colonies modeled as an ensemble of spheres embedded at the periphery of a spherical ECM were also considered. Interestingly, the impact of mutual shading on the average mass absorption cross-section was similar for both cell arrangements despite differences in the volume fraction $f_v = N_c r_c^3 / r_{ECM}^3$ occupied by the cells ranging from 0.83 to 0.98 for fractal colonies and from 0.14 to 0.41 for ordered spherical colonies. This suggests that mutual shading may impact the average cell absorption cross-section even at low volume fractions f_v like those observed for *Volvocaceae* including *Eudorina* for which f_v ranges from 0.04 to 0.15 [4,43].

This study aims to predict, for the first time, the spectral absorption cross-section of microalgae colonies of the genus *Eudorina* as a representative case. As a member of the *Volvocaceae* family, *Eudorina* shares similarities with a variety of other colonial microalgae in terms of cell size, structure, and colony structure [2,48]. Furthermore, among the *Volvocaceae*, the morphology of *Eudorina* colonies represents an average case in terms of colony radius and number of constituent cells [48,49]. To predict their absorption cross-section, these colonies were represented as large, absorbing, optically soft (i.e., weakly refracting) equidistant monodisperse spherical cells embedded at the periphery of a refracting but non-absorbing spherical extracellular matrix. The MCRT method was first validated by comparing, whenever possible, its predictions of the absorption cross-section of an ensemble of optically soft particles with those by the superposition T-matrix method. It was then used to simulate absorption in the PAR region for realistic colony dimensions where the superposition T-matrix method could not be used due to the excessively large cell and ECM size parameters. The effects of the absorption index, radius, and number of photosynthetic cells in the colonies were investigated to gain a better understanding of their interaction with light and of the importance of shading effects.

2. Analysis

2.1. Problem statement

Eudorina colonies are comprised of 16, 32, and 64 photosynthetic cells approximately equidistant and arranged at the periphery of a spherical ECM. A detailed discussion of the morphologies and the number of cells in these colonies can be found elsewhere [4,43–45] and need not be repeated. Fig. 2 depicts a representative case of the idealized morphology of a *Eudorina* colony for the purpose of simulating their interaction with light. Here, the colony consisted of a large spherical ECM of radius $r_{ECM} = 60$ μm encompassing $N_c = 64$ monodisperse equidistant spherical reproductive photosynthetic cells of radius $r_c = 8$ μm. These dimensions were chosen based on experimental observations reported in the literature [4,43–45], as previously discussed. In general, the colonies simulated contained 16, 32, or 64 cells corresponding to cell volume fractions f_v equal to 0.04, 0.08, and 0.15, respectively. Cell radius r_c ranged from 5 to 13 μm. The ECM radius r_{ECM} scaled with the cell radius r_c such that the volume fraction f_v was constant for a given number of cells N_c and equal to that of the colony shown in Fig. 2, i.e., $r_{ECM} = (60/8) r_c$. The centers of the cells were located on the surface of an inner concentric sphere of radius $r_i = r_{ECM} - r_c$. Their positions were generated using a program developed for uniform triangular tessellation of sampling points on the surface of a sphere [50].

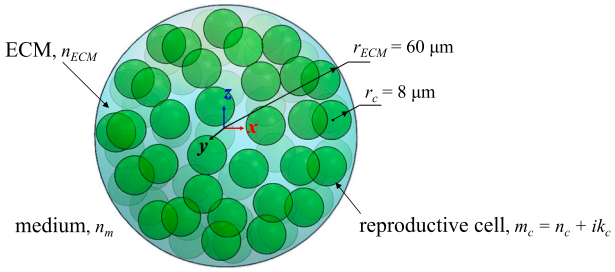

Fig. 2. Schematic of the simulated idealized colony of *Eudorina* comprised of $N_c = 64$ photosynthetic cells with complex index of refraction $m_c = n_c + ik_c$ and radius $r_c = 8$ μm embedded within a non-absorbing extracellular matrix (n_{ECM}) of radius $r_{ECM} = 60$ μm surrounded by non-absorbing medium (n_m).

The refractive index of the non-absorbing surrounding medium n_m was assumed to be that of water, i.e., $n_m = 1.333$ [51]. The refractive index of the non-absorbing ECM was taken as $n_{ECM} = 1.36$ corresponding to glycoprotein hydroxyproline [49,52], one of the main constituents found in the ECM of *Volvocaceae* [53]. Unless otherwise noted, the complex index of refraction of the photosynthetic cell was taken as $m_c = n_c + ik_c = 1.355 + i0.004$. These values were representative of various microalgae species around the Chlorophyll *a* absorption peak in the PAR region [16,27,34]. Note that in the PAR region, the absorption index k_c of photosynthetic microalgae cells, including *C. reinhardtii*, is typically less than 0.007 [16,27,34]. The resulting relative refractive index of the ECM was $n_{ECM}/n_m = 1.0203$ and that of the cells was $m_c/n_{ECM} = 0.9963 + i0.003$, corresponding to optically soft scatterers. The size parameter $x_{ECM} = 2\pi r_{ECM}/\lambda$ of the simulated colonies ranged from 500 to 900.

2.2. Prediction of radiation characteristics of microalgae colonies

The absorption cross-section C_{abs} (in μm^2) of the ensemble of spheres was predicted using either the superposition T-matrix code developed by Mackowski and Mishchenko [54] or the Monte Carlo ray-tracing method developed in Ref. [35]. The T-matrix method and algorithm have been described in detail in Refs. [54–56] and need not be repeated. In brief, the superposition T-matrix method estimates the scattered electromagnetic (EM) field from an ensemble of spheres by superposing the scattered EM fields from each of the constituting spheres or monomers [55,56]. Initially, the vector spherical harmonic expansion of the scattered and internal EM fields of each sphere is written about the sphere's origin. The EM field incident on each sphere consists of the external incident field reaching the sphere and the scattered fields from all other spheres in the ensemble. Then, the system of equations for unknown scattering coefficients is inverted to obtain the T-matrix [55,56]. Finally, using an analytical rotation transformation rule to integrate the incident EM field over every propagation direction, the unitless scattering Q_{sca} and extinction Q_{ext} efficiency factors are obtained from operations on the T-matrix [55,56]. Then, the absorption efficiency factor Q_{abs} is given by $Q_{abs} = Q_{ext} - Q_{sca}$.

The Monte Carlo ray-tracing method (MCRT) models light transfer through an ensemble of spheres and colonies by tracking a large number

of discrete photon bundles or "rays". This method is valid when the size parameter x and phase shift parameter $|m-1|x$ of the scatterer are much larger than unity and geometric optics prevails, i.e., $x \gg 1$ and $|m-1|x \gg 1$, where m is the relative complex index of refraction of the absorber/scatterer. The method and algorithm have been described in detail in Ref. [35] and need not be repeated. In brief, the path of each incident ray was tracked through the colony. At each medium/ECM and ECM/cell interface the probability of reflection or refraction was determined by Fresnel's equations and the direction of the refracted rays by Snell's law. The ray path length l_p through the absorbing cells was recorded and used to calculate the transmissivity τ for a given ray path according to $\tau = exp(-\kappa_c l_p)$ where the cell absorption coefficient κ_c (in m^{-1}) is given by $\kappa_c = 4\pi k_c/\lambda$. Then, a random number between 0 and 1 was generated and compared to the value of τ to determine if the ray was absorbed or transmitted. The number of rays N_{abs} absorbed by the colony and the total number of rays N_{in} incident on the colony were counted to obtain the absorption efficiency factor Q_{abs} given by

$$Q_{abs} = \frac{N_{abs}}{N_{in}} \tag{1}$$

Here, the number of rays N_{in} sufficient to achieve numerical convergence was 10^6 (see Fig. S1 in Supplementary Materials). In both methods, the absorption cross-section C_{abs} of the colony can be calculated from the computed absorption efficiency factor Q_{abs} according to [57]

$$C_{abs} = Q_{abs}\pi r_{ECM}^2 \tag{2}$$

Finally, the mass absorption cross-section A_{abs} (in m^2kg^{-1}) can be calculated using the colony absorption-cross section C_{abs} according to [35,58]

$$A_{abs,\lambda} = \frac{C_{abs,\lambda}}{V\rho_{dm}(1-x_w)N_c} \tag{3}$$

where V is the cell volume, ρ_{dm} is the dry material density of biomass taken as 1350 kg m^{-3}, and x_w is the cell water fraction taken as 0.78. These values were taken from the literature for *C. reinhardtii* due to its close genetic relation to *Eudorina* [2,48,49].

As discussed previously, the superposition T-matrix method can be resource-intensive, particularly as the size of the colony and/or the number of photosynthetic cells therein increases. Indeed, the amount of RAM required to predict the absorption cross-section C_{abs} of *Eudorina* colonies via the T-matrix method increased exponentially with increasing ECM r_{ECM} and/or cell r_c radius for a given wavelength λ (see Fig. S2 in Supplementary Materials). Therefore, the maximum ECM size parameter simulated by this method was limited computationally to $x_{ECM} \leq 500$ which required up to 2.6 TB of RAM. On the other hand, the MCRT method could simulate colonies with larger ECM size parameters using a personal computer with an 8-core CPU and 8 GB of RAM.

3. Results and discussion

3.1. Numerical validation

Fig. 3 compares the absorption cross-section C_{abs} (in μm^2) of an ensemble of 64 equidistant spherical cells distributed on a concentric sphere surface within a non-absorbing spherical ECM, analogous to the colonies described previously, predicted by the superposition T-matrix and by the Monte Carlo ray-tracing methods as a function of the cell r_c and ECM r_{ECM} radii such that $r_{ECM} = (60/8)r_c$, as previously discussed. The wavelength λ of the incident radiation was equal to 676 nm. The size parameters of the cell x_c and of the ECM x_{ECM} ranged from 0.13 to 67 and from 1 to 500, respectively. Here, the cell phase shift parameter $|m-1|x_c$ ranged from 4.8×10^{-4} to 0.25 and the ECM phase shift parameter $|m-1|x_{ECM}$ ranged from 0.02 to 10. Fig. 3 demonstrates that the

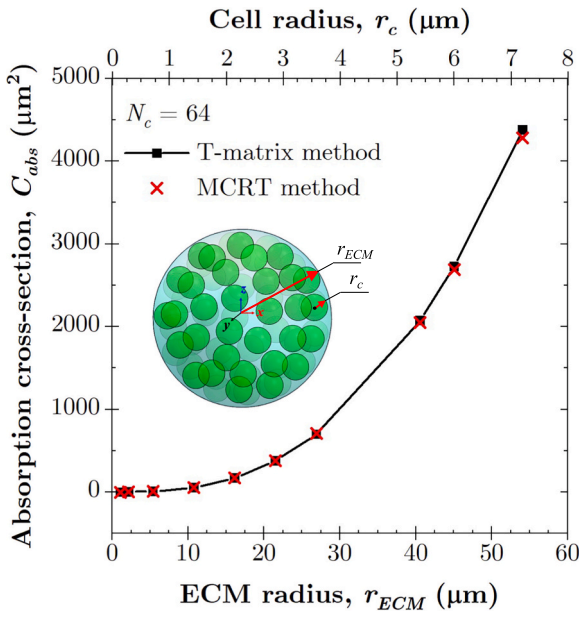

Fig. 3. Validation of the Monte Carlo ray-tracing (MCRT) method in predicting the absorption cross-section C_{abs} of an ensemble of 64 cells as a function of ECM r_{ECM} and cell r_c radius with $r_{ECM} = (60/8)r_c$ against predictions by the superposition T-matrix.

absorption cross-section C_{abs} predicted by the superposition T-matrix method and by the Monte Carlo ray-tracing method were in excellent agreement. In fact, the relative difference between the two methods was less than 2.2 % over the simulated range of cell r_c and ECM r_{ECM} radii. This was the case despite the fact that the superposition T-matrix method accounted for diffraction effects while the MCRT method did not. This suggests that diffraction effects did not impact light absorption by an ensemble of optically soft spheres, despite playing an important role in their scattering cross-sections. Indeed, due to diffraction effects, the scattering cross-section of the colonies simulated in Fig. 3 could not be predicted by the MCRT, as illustrated in Fig. S3 of Supplementary Materials. This observation was also made for colonies consisting of fractal aggregates of cells in a spherical ECM, as previously discussed [35].

Overall, these results validate the MCRT method for modeling light absorption by an ensemble of optically soft spheres even though the conditions for which geometric optics is valid were not rigorously satisfied, namely $x \gg 1$ and $|m-1|x \gg 1$. This indicates that the MCRT method can serve as an alternative to the superposition T-matrix method for modeling light absorption by an ensemble of large optically soft spheres. Here, the MCRT method was used to predict the absorption cross-section of *Eudorina* colonies over the PAR region since their ECM size parameter x_{ECM} exceed 900 and was prohibitively large for the superposition T-matrix method.

3.2. Effect of shading

Fig. 4a plots the absorption cross-section C_{abs} predicted by the MCRT method as a function of the radii r_{ECM} of the ECM and r_c of the cells for *Eudorina* colonies with 16, 32, and 64 constituent cells. The wavelength λ of the incident radiation was equal to 678 nm corresponding to one of the absorption peaks of Chlorophyll *a*. Fig. 4a indicates that the predicted absorption cross-section C_{abs} increased with increasing cell number N_c and radius r_c. This was due to the associated increase in the volume of absorbing substance (i.e., the cells) and in the projected area πr_{ECM}^2 of the colony. Fig. 4b plots the colony mass absorption cross-section C_{abs} normalized with respect to the product of the number of cells N_c and the absorption cross-section C_{abs}^{cc} of a culture featuring single

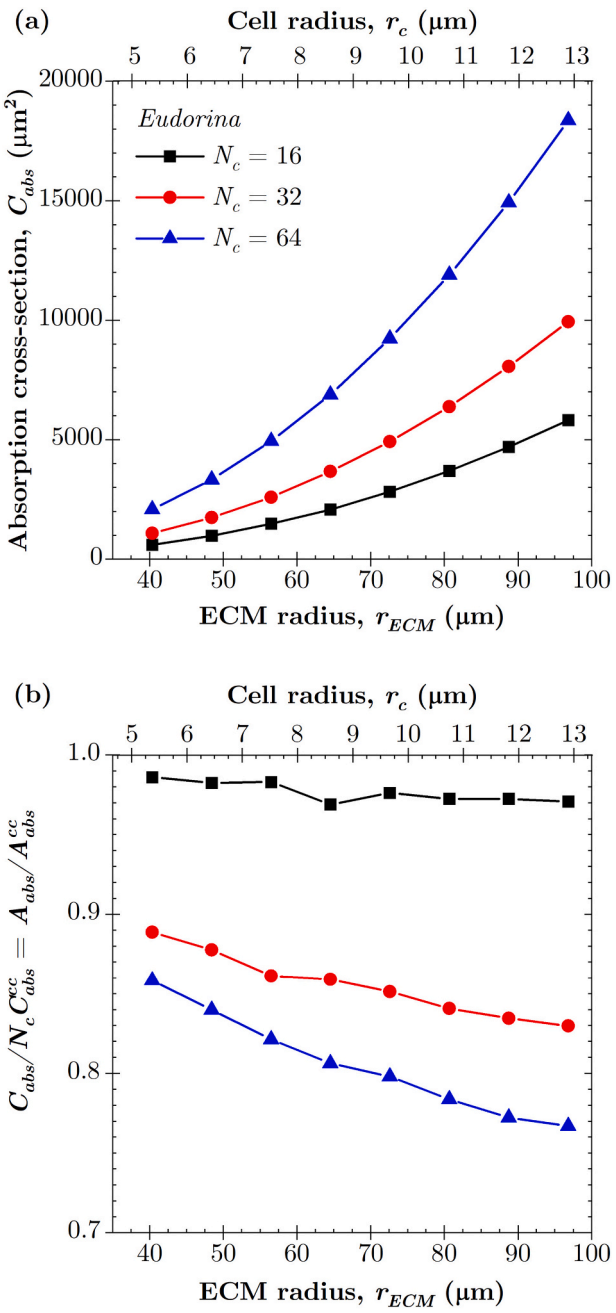

Fig. 4. (a) Absorption cross-section C_{abs} of *Eudorina* colonies and (b) normalized mass absorption cross-section $C_{abs}/N_cC^{cc}_{abs} = A_{abs}/A^{cc}_{abs}$ predicted by the Monte Carlo ray-tracing method as functions of the ECM r_{ECM} and cell r_c radii for *Eudorina* colonies with number of cells N_c equal to 16, 32, and 64.

cells of radius r_c coated with an ECM shell of radius r_{ECM} equal to that of the colonies. The single cells were considered to be within an ECM for normalizing the colony absorption cross-section so as to account for reflection and refraction at the medium/ECM interface. Note that a ratio of $C_{abs}/N_cC^{cc}_{abs} = A_{abs}/A^{cc}_{abs}$ equal to unity would indicate that the colony absorption cross-section is unaffected by colony formation. In this case, the absorption cross-section C_{abs} can be approximated as the sum of the absorption cross-sections of the constituent cells, i.e., $C_{abs} = N_cC^{cc}_{abs}$. Then, mutual shading among cells in the colony would be negligible. This was approximately the case for colonies with $N_c = 16$ where cells were the least densely packed. However, for colonies with a number of cells $N_c \geq 32$, the ratio $C_{abs}/N_cC^{cc}_{abs} = A_{abs}/A^{cc}_{abs}$ was less than unity and decreased with increasing number of cells N_c for given cell r_c or ECM r_{ECM} radii. Indeed, compared to a single coated cell, individual cells in a colony with $N_c = 64$ absorbed, on average, up to 23 % less light due to mutual shading among cells. Finally, the ratio $C_{abs}/N_cC^{cc}_{abs} = A_{abs}/A^{cc}_{abs}$ also decreased with increasing cell radius r_c. This observation indicates that the impact of mutual shading was stronger for larger cells (see Fig. 4a) since absorption is a volumetric process.

3.3. *Eudorina* spectral absorption cross-section

Fig. 5a plots the spectral absorption cross-section $C_{abs,\lambda}$ over the PAR region for *Eudorina* colonies with 16, 32, or 64 constituent cells with ECM radius $r_{ECM} = 60$ μm and cell radius $r_c = 8$ μm (Fig. 2). The spectral absorption cross-section of a single coated cell C^{cc}_{abs} is also shown for reference as $N_c = 1$. Here, the spectral absorption index $k_{c,\lambda}$ of the cells was estimated according to [36,58]

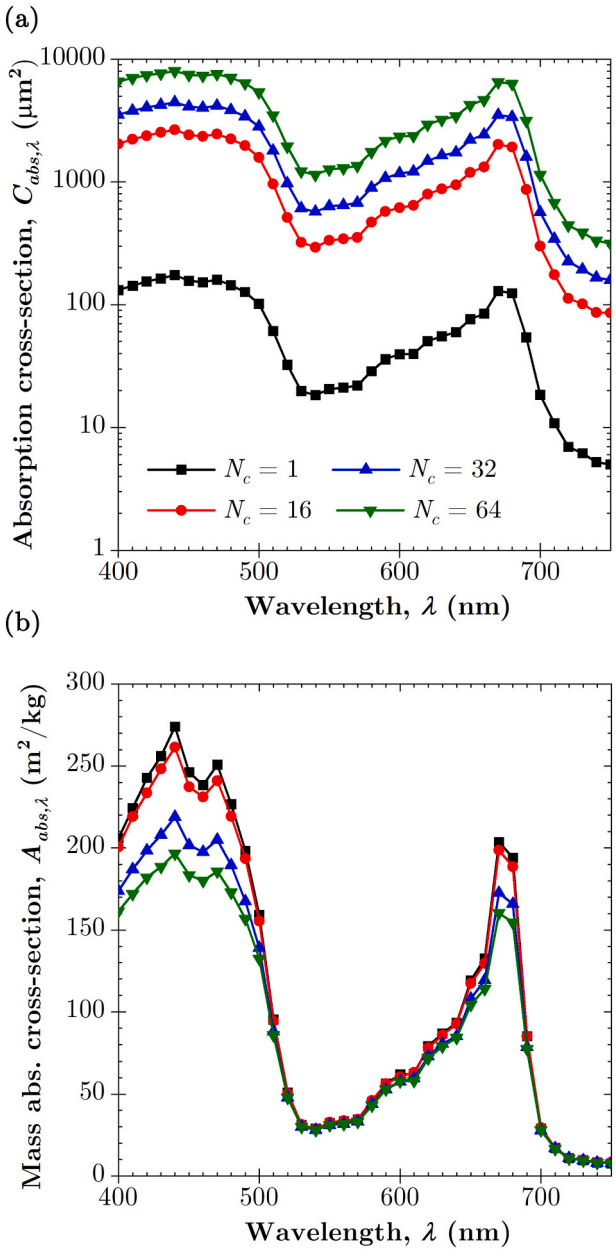

Fig. 5. (a) Spectral absorption cross-section $C_{abs,\lambda}$ and (b) spectral mass absorption cross-section $A_{abs,\lambda}$ of *Eudorina* colonies over the PAR region for $r_{ECM} = 60$ μm and $r_c = 8$ μm and number of cells N_c equal to 1, 16, 32, and 64.

$$k_{c,\lambda} = \frac{\lambda}{4\pi}\sum_i C_i Ea_{i,\lambda} = \frac{\lambda}{4\pi}\rho_{dm}(1-x_w)w_{pig}\sum_i x_i Ea_{i,\lambda} \quad (4)$$

where C_i is the concentration of the i^{th} pigment in the cell (in g L^{-1}) and $Ea_{i,\lambda}$ is the specific absorption cross-section (in m^2kg^{-1}) of a given pigment as reported in Ref. [59]. Here, w_{pig} is the total pigment concentration (in %) on a dry biomass basis and x_i is the mass fraction of the i^{th} pigment based on the total pigment mass. Pigment concentrations reported for *Chlamydomonas reinhardtii* were used for *Eudorina* since they are close genetic relatives [2] and corresponded to total pigment concentration $w_{pig} = 2.55$ % and pigment mass fractions x_i of 55 %, 27.4 %, and 17.6 % for Chl. *a*, *b*, and photoprotective carotenoids, respectively. The cell and ECM refractive indices, n_c and n_{ECM}, were assumed to be constant over the PAR region [35]. Fig. 5a shows a clear increase in the spectral absorption cross-section $C_{abs,\lambda}$ of the colonies with increasing number of cells N_c and absorption peaks corresponding to those of Chlorophyll *a* at 437 nm and 678 nm and Chlorophyll *b* at 475 nm.

Fig. 5b plots the corresponding spectral colony mass absorption cross-section $A_{abs,\lambda}$ (in m^2kg^{-1}) over the PAR region. Here, $A_{abs,\lambda}$ was calculated using the colony spectral absorption-cross section $C_{abs,\lambda}$ shown in Fig. 5a. Fig. 5b indicates that the spectral mass absorption cross-section decreased with increasing number of cells due to mutual shading. This effect was more pronounced at the absorption peaks of Chl. *a* and Chl. *b* where the absorption index $k_{c,\lambda}$ was the largest, resulting in increased shading. Indeed, neglecting shading effects would overestimate the colony absorption cross-section by as much as 37 % for the colony containing 64 cells at wavelength $\lambda = 420$ nm. On the other hand, the spectral mass absorption cross-section $A_{abs,\lambda}$ defined per unit of biomass was independent of the number of cells present for wavelengths λ between 500 and 650 nm and greater than 700 nm when the cells were weakly absorbing ($k_{c,\lambda} \leq 2.6\times\ 10^{-3}$) and shading effects were negligible.

Fig. 6a plots the spectral mass absorption cross-section $A_{abs,\lambda}$ of a colony-containing culture with a number of cells per colony $N_c = 64$ normalized by the spectral mass absorption cross-section for a single coated cell $A^{cc}_{abs,\lambda}$ for total pigment concentrations w_{pig} equal to 2 %, 4 %, and 6 %. As discussed previously, a ratio of $A_{abs,\lambda}/A^{cc}_{abs,\lambda}$ equal to unity would indicate that $A_{abs,\lambda}$ was unaffected by the presence of colonies. However, Fig. 6a shows that shading among cells in the colonies caused the ratio $A_{abs,\lambda}/A^{cc}_{abs,\lambda}$ to be less than unity over the PAR region, particularly near the absorption peaks of Chl. *a* and *b*.

Fig. 6b plots the ratio of A_{abs}/A^{cc}_{abs} at wavelength $\lambda = 440$ nm corresponding to one of the absorption peaks of Chl. *a* as a function of the total pigment concentration w_{pig} for colonies with 16, 32, or 64 cells. Notably, for a colony with $N_c = 16$, Fig. 6b indicates that the ratio A_{abs}/A^{cc}_{abs} was nearly independent of pigment concentration. Then, increasing pigment concentration did not increase mutual shading among colonies with $N_c = 16$. This can be attributed to their less densely-packed colony structure and lower volume fraction $f_v = 0.04$ which limited shading among the cells even when the cell absorption index k_c was large. For colonies with N_c equal to 32 or 64, the ratio A_{abs}/A^{cc}_{abs} decreased with increasing pigment concentration. In this case, the cells were more densely packed and the impact of mutual shading increased with increasing pigment concentration.

3.4. Light transfer in microalgae cultures

To assess the impact of colony formation on light transfer within microalgae cultures, the local rate of photon absorption (LRPA) $\mathscr{A}(z)$ (in $\mu mol_{h\nu}\,g^{-1}s^{-1}$) was calculated according to

$$\mathscr{A}(z) = \int_{PAR} A_{abs,\lambda} G_\lambda(z) d\lambda \quad (5)$$

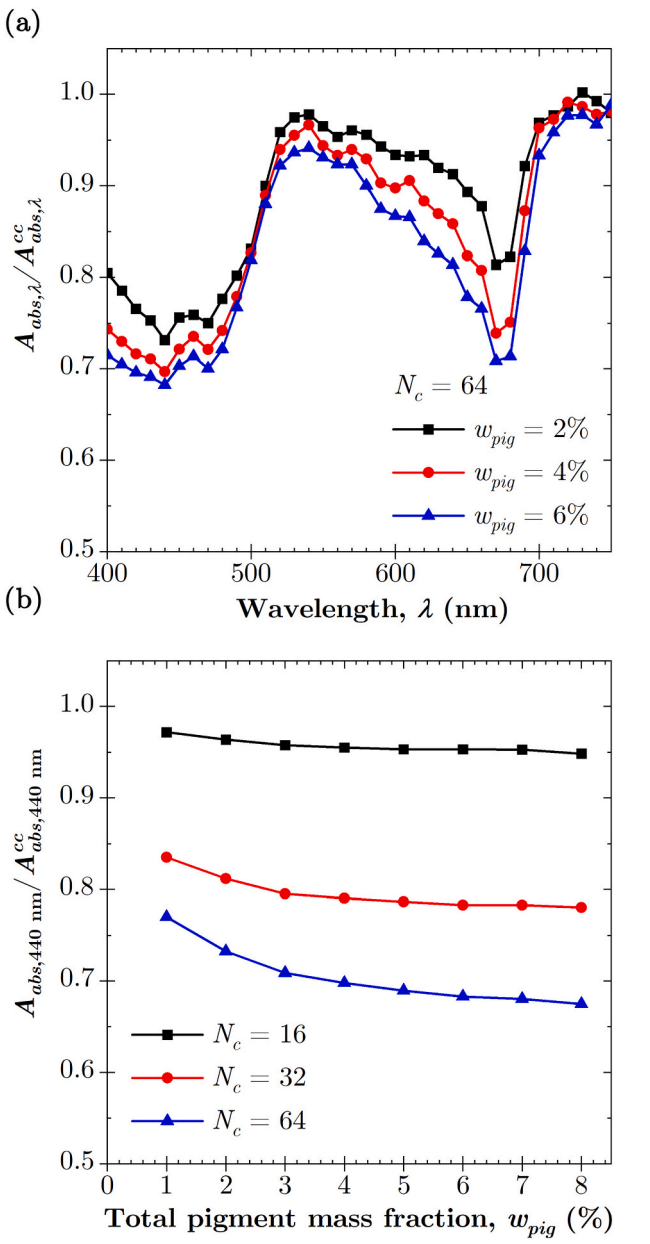

Fig. 6. (a) Spectral normalized mass absorption cross-section $A_{abs,\lambda}/A^{cc}_{abs,\lambda}$ for a colony-containing culture with $N_c = 64$ and pigment concentration w_{pig} equal to 2 %, 4 %, and 6 % and (b) normalized mass absorption cross-section $A_{abs,440\ nm}/A^{cc}_{abs,440\ nm}$ as a function of pigment concentration for colonies containing $N_c =$ 16, 32, and 64.

the local spectral fluence rate $G_\lambda(z)$ (in $\mu mol_{h\nu}\,m^{-2}s^{-1}$) for a PBR with a transparent back wall was estimated using a simplified method proposed by Kandilian et al. [22]

$$G_\lambda(z) = q'_{in} e^{-A_{abs,\lambda}C_x z} \quad (6)$$

Here, C_x is the culture biomass concentration (in g L^{-1}) and q'_{in} represents the incident photon flux density consisting of white, collimated, normally incident, light such that $q'_{in} = 200\ mol_{h\nu}m^{-2}s^{-1}$. The spectral mass absorption cross-sections $A_{abs,\lambda}$ for cultures featuring single cells or colonies with 16, 32, or 64 cells shown in Fig. 5b were used. The culture depth was 4 cm and representative of a laboratory-scale PBR [60].

Figs. 7a-c show the resulting LRPA for cultures with a pigment

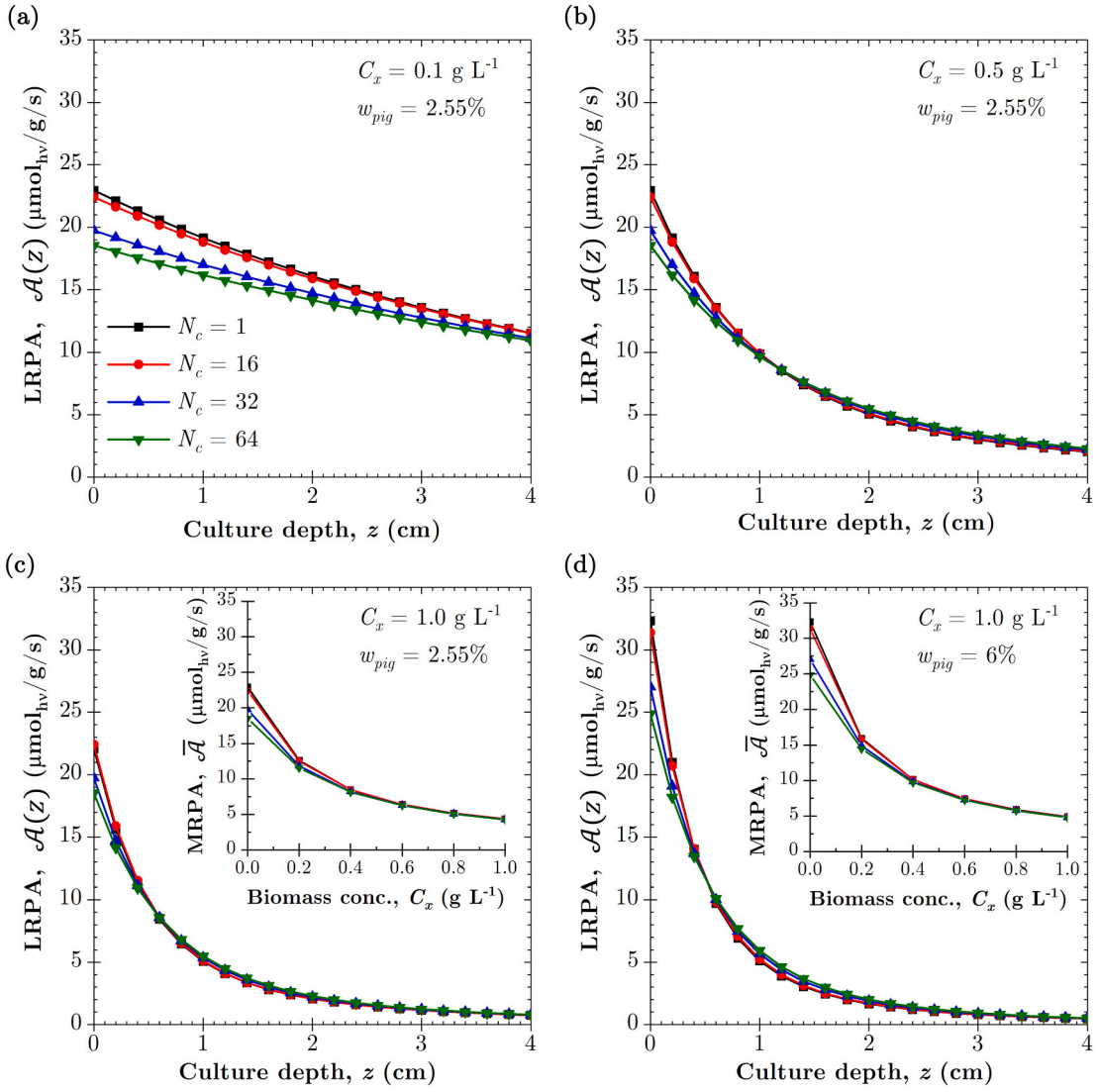

Fig. 7. Local rate of photon absorption (LRPA) $\mathscr{A}(z)$ as a function of culture depth for pigment concentration $w_{pig} = 2.55$ % and biomass concentration C_x of (a) 0.1, (b) 0.5, and (c) 1.0 g L^{-1} and (d) for $w_{pig} = 6$ % and $C_x = 1.0$ g L^{-1}. The MRPA as a function of biomass concentration C_x is also shown for w_{pig} equal to (c) 2.55 % and (d) 6 %. Cultures containing isolated cells or colonies with N_c equal to 16, 32, or 64 were considered.

concentration $w_{pig} = 2.55$ % featuring single cells or colonies with 16, 32, or 64 cells and for biomass concentrations C_x of (a) 0.1, (b) 0.5, and (c) 1.0 g L^{-1}, respectively. Fig. 7d also shows $\mathscr{A}(z)$ but for a larger pigment concentration of $w_{pig} = 6$ % and biomass concentration $C_x = 1.0$ g L^{-1}. Fig. 7a indicates that at low biomass concentrations, the LRPA $\mathscr{A}(z)$ decreased with increasing number of cells N_c present in the colonies. Indeed, localized shading within the colonies decreased the amount of light absorbed by the culture compared to a culture featuring isolated cells with the same biomass concentration.

For larger biomass concentrations, Fig. 7b and 7c indicate that colony formation decreased the LRPA only at shallower culture depths. For example, at biomass concentration $C_x = 0.5$ g L^{-1}, Fig. 7b illustrates a decrease in the LRPA for cultures containing colonies, but only up to a culture depth of approximately 1.2 cm. Beyond this depth, the LRPA was slightly larger for colony-containing cultures. This was due to their smaller mass absorption cross-section $A_{abs,\lambda}$ (Fig. 5b) which reduced the amount of light absorbed near the culture surface and resulted in deeper light penetration into the culture. Similarly, the LRPA was slightly larger for colony-containing cultures at depths $z > 1.2$ cm thanks to the increase in the local fluence rate $G_\lambda(z)$ and despite the smaller mass absorption-cross section $A_{abs,\lambda}$. Nonetheless, at biomass concentration $C_x = 0.5$ g L^{-1}, the net effect was a decrease in the MRPA by up to 4 % for a culture comprised of colonies of 64 cells compared to one comprised of single cells.

Fig. 7c and 7d compare the LRPA as a function of culture depth z and the mean rate of photon absorption (MRPA) as a function of biomass concentration C_x for pigment concentration w_{pig} equal to 2.55 % and 6 %, respectively. Fig. 7c and 7d indicate that larger pigment concentrations increased the LRPA at shallow culture depths and increased the MRPA at lower biomass concentrations for all colony configurations. The insets in Fig. 7c and 7d also demonstrate that the MRPA decreased in the presence of colonies, particularly at low biomass concentrations. Indeed, at biomass concentration $C_x = 0.1$ g L^{-1}, the MRPA of cultures comprised of colonies of 64 cells was 13.1 % and 15.6 % smaller than that of a culture of comprised of single cells for pigment concentrations w_{pig} of 2.55 % and 6 %, respectively. Such a decrease in light absorbed would have a negative impact on the photosynthetic growth rate. By contrast, for biomass concentrations larger than 0.5 g L^{-1}, the impact of colony formation was negligible.

Overall, this study indicates that the morphology of microalgae colonies plays an important role in their interaction with light. Mutual shading among cells was shown to decrease their mass average spectral

absorption cross-section $A_{abs,\lambda}$. The same effect will occur in any colony-forming species such as those of the *Volvocaceae* family which are found in algal blooms [6–9]. Thus, for a given pigment concentration, an algae bloom of colony-forming species may absorb less light than one containing single cells. This could impact the interpretation of reflectance data used in remote sensing of chlorophyll content in algae blooms [14,15]. Furthermore, the quantity of photons absorbed by the cells is directly related to the algae growth rate [21]. Here, we showed that colony formation can decrease the mean rate of photon absorption MRPA. Thus, mitigating colony formation and/or accounting for the impacts of shading will be important for optimizing the design and operation of photobioreactors used for cultivating colony-forming microalgae.

4. Conclusion

The absorption cross-sections of colonial microalgae *Eudorina* consisting of 16, 32, and 64 equidistant absorbing photosynthetic cells distributed on a concentric sphere surface within a non-absorbing spherical extracellular matrix (ECM) were computed using the Monte Carlo ray-tracing method. The latter was validated against the superposition T-matrix method for modeling absorption by an ensemble of optically soft particles. At wavelengths where the cells were weakly absorbing, the absorption cross-section of colonies was equivalent to the cumulative absorption cross-sections of individual cells coated by an ECM with the same radius as the colonies. However, in the spectral range where cells absorb, the impact of shading effects on the colony absorption cross-section increased with increasing cell radius, number of cells, and cell absorption index. Furthermore, colony formation was found to decrease the local and mean rate of photon absorption in a microalgae culture, particularly at low biomass concentration. The implication of these findings for remote sensing of phytoplankton blooms and design and operation of PBRs were discussed. From a radiation transfer standpoint, the MCRT method proved to be an efficient and accurate tool for predicting the spectral absorption cross-section of colonies, capable of accurately capturing the impact of shading among cells.

CRediT authorship contribution statement

Jack Hoeniges: Methodology, Software, Validation, Investigation, Visualization, Writing – original draft. **Arka Bhowmik:** Conceptualization, Investigation, Visualization, Writing – original draft. **Refet A. Yalçin:** Methodology, Software, Validation, Resources, Writing – review & editing. **Vincent J. Partusch:** Resources, Visualization, Writing – review & editing. **Laurent Pilon:** Conceptualization, Supervision, Funding acquisition, Writing – review & editing.

Declaration of competing interest

The authors declare that they have no known competing financial interests or personal relationships that could have appeared to influence the work reported in this paper.

Data availability

Data will be made available on request.

Acknowledgment

JH acknowledges financial support from the National Science Foundation NRT-INFEWS: Integrated Urban Solutions for Food, Energy, and Water Management (Grant No. DGE-1735325).

Appendix A. Supplementary materials

Supplementary material to this article can be found online at https://doi.org/10.1016/j.algal.2023.103082.

References

[1] L. Barsanti, P. Gualtieri, Algae: Anatomy, Biochemistry, and Biotechnology, CRC Press, Boca Raton, FL, 2014.
[2] I. Nishii, S.M. Miller, Volvox: simple steps to developmental complexity? Curr. Opin. Plant Biol. 13 (6) (2010) 646–653.
[3] J. Beardall, D. Allen, J. Bragg, Z.V. Finkel, K.J. Flynn, A. Quigg, T.A.V. Rees, A. Richardson, J.A. Raven, Allometry and stoichiometry of unicellular, colonial and multicellular phytoplankton, New Phytol. 181 (2) (2008) 295–309.
[4] S.F. Gilbert, Developmental Biology, Sinauer Associates, Sunderland, MA, 2014.
[5] C.B. Lopez, Q. Dortch, E.B. Jewett, D. Garrison, Scientific Assesement of Marine Harmful Algal Blooms, Interagency Working Group on Harmful Algal Blooms, Hypoxia, and Human Health of the Joint Subcommittee on Ocean Science and Technology, Washington, D.C., 2008.
[6] H.W. Paerl, Nuisance phytoplankton blooms in coastal, estuarine, and inland waters, Limnol. Oceanogr. 33 (1988) 823–843.
[7] J. Kiss, Investigation of the water blooms of Eudorina elegans in the dead-arm of the river tisza at the community Mártély, Tiscia (Szeged) 12 (1977) 37–47.
[8] P. Znachor, J. Jezberová, The occurrence of a bloom-forming green alga Pleodorina indica (Volvocales) in the downstream reach of the river Malše (Czech Republic), Hydrobiologia 541 (2005) 221–228.
[9] M.I. Gladyshev, N.N. Sushchik, G.S. Kalachova, L.A. Shchur, The effect of algal blooms on the disappearance of phenol in a small forest pond, Water Res. 32 (9) (1998) 2769–2775.
[10] C.N. Sawyer, The need for nutrient control, J. Water Pollut. Control Fed. 40 (3) (1968) 363–370.
[11] E.A. Sigworth, Control of odor and taste in water supplies, Am. Water Works Assoc. 49 (12) (1957) 1507–1521.
[12] D. Blondeau-Patissier, J.F.R. Gower, A.G. Dekker, S.R. Phinn, V.E. Brando, A review of ocean color remote sensing methods and statistical techniques for the detection, mapping and analysis of phytoplankton blooms in coastal and open oceans, Prog. Oceanogr. 123 (2014) 123–144.
[13] S.C.J. Palmer, D. Odermatt, P.D. Hunter, C. Brockmann, M. Présing, H. Balzter, V. R. Tóth, Satellite remote sensing of phytoplankton phenology in Lake Balaton using 10 years of MERIS observations, Remote Sens. Environ. 158 (2015) 441–452.
[14] T. Kutser, Quantitative detection of chlorophyll in cyanobacterial blooms by satellite remote sensing, Limnol. Oceanogr. 49 (6) (2004) 2179–2189.
[15] S. Sathyendranath, G. Cota, V. Stuart, H. Maass, T. Platt, Remote sensing of phytoplankton pigments: a comparison of empirical and theoretical approaches, Int. J. Remote Sens. 22 (2–3) (2001) 249–273.
[16] M. Jonasz, G. Fournier, Light Scattering by Particles in Water: Theoretical and Experimental Foundations, Academic Press, San Diego, CA, 2007.
[17] F. Zhang, M. Prigge, F. Beyrière, S.P. Tsunoda, J. Mattis, O. Yizhar, P. Hegemann, K. Deisseroth, Red-shifted optogenetic excitation: a tool for fast neural control derived from Volvox carteri, Nat. Neurosci. 11 (6) (2008) 631–633.
[18] L.G. Lowder, S.K. Herbert, Heterologous expression of a volvox cell adhesion molecule causes flocculation in Chlamydomonas reinhardtii, J. Appl. Phycol. 27 (2) (2015) 721–731.
[19] C.J. Tien, D.C. Sigee, K.N. White, Copper adsorption kinetics of cultured algal cells and freshwater phytoplankton with emphasis on cell surface characteristics, J. Appl. Phycol. 17 (5) (2005) 379–389.
[20] B. Podola, M. Melkonian, Selective real-time herbicide monitoring by an array chip biosensor employing diverse microalgae, J. Appl. Phycol. 17 (3) (2005) 261–271.
[21] J. Pruvost, J.-F. Cornet, Knowledge models for the engineering and optimization of photobioreactors, in: C. Posten, W. Christian (Eds.), Microalgal Biotechnology: Potential and Production, De Gruyter, Berlin, DE, 2012, pp. 181–224, chapter 10.
[22] R. Kandilian, A. Soulies, J. Pruvost, B. Rousseau, J. Legrand, L. Pilon, Simple method for measuring the spectral absorption cross-section of microalgae, Chem. Eng. Sci. 146 (jun 2016.) 357–368.
[23] E. Lee, J. Pruvost, X. He, R. Munipalli, L. Pilon, Design tool and guidelines for outdoor photobioreactors, Chem. Eng. Sci. 106 (2014) 18–29.
[24] A. Bricaud, A.L. Bédhomme, A. Morel, Optical properties of diverse phytoplanktonic species: experimental results and theoretical interpretation, J. Plankton Res. 10 (5) (1988) 851–873.
[25] H. Berberoğlu, L. Pilon, Experimental measurements of the radiation characteristics of Anabaena variabilis ATCC 29413-U and rhodobacter sphaeroides ATCC 49419, Int. J. Hydrog. Energy 32 (18) (2007) 4772–4785.
[26] H. Berberoğlu, L. Pilon, A. Melis, Radiation characteristics of Chlamydomonas reinhardtii CC125 and its truncated chlorophyll antenna transformants tla1, tlaX and tla1-CW+, Int. J. Hydrog. Energy 33 (22) (2008) 6467–6483.
[27] E. Lee, R.L. Heng, L. Pilon, Spectral optical properties of selected photosynthetic microalgae producing biofuels, J. Quant. Spectrosc. Radiat. Transf. 114 (2013) 122–135.
[28] C.Y. Ma, J.M. Zhao, L.H. Liu, L. Zhang, X.C. Li, B.C. Jiang, GPU-accelerated inverse identification of radiative properties of particle suspensions in liquid by the Monte Carlo method, J. Quant. Spectrosc. Radiat. Transf. 172 (2016) 146–159.
[29] A. Bricaud, A. Morel, Light attenuation and scattering by phytoplanktonic cells: a theoretical modeling, Appl. Opt. 25 (4) (1986) 571.

[30] D. Stramski, A. Bricaud, A. Morel, Modeling the inherent optical properties of the ocean based on the detailed composition of the planktonic community, Appl. Opt. 40 (18) (2001) 2929.
[31] A. Bhowmik, L. Pilon, Can spherical eukaryotic microalgae cells be treated as optically homogeneous? J. Opt. Soc. Am. A 33 (8) (2016) 1495–1503.
[32] E. Lee, L. Pilon, Absorption and scattering by long and randomly oriented linear chains of spheres, J. Opt. Soc. Am. A 30 (9) (2013) 1892–1900.
[33] R.L. Heng, K.C. Sy, L. Pilon, Absorption and scattering by bispheres, quadspheres, and circular rings of spheres and their equivalent coated spheres, J. Opt. Soc. Am. A 32 (1) (2015) 46.
[34] R. Kandilian, R.L. Heng, L. Pilon, Absorption and scattering by fractal aggregates and by their equivalent coated spheres, J. Quant. Spectrosc. Radiat. Transf. 151 (2015) 310–326.
[35] J. Hoeniges, R. Kandilian, C. Zhang, J. Pruvost, J. Legrand, D. Grizeau, L. Pilon, Effect of colony formation on light absorption by Botryococcus braunii, Algal Res. 50 (2020), 101985.
[36] L. Pilon, R. Kandilian, Interaction between light and photosynthetic microorganisms, in: J. Legrand (Ed.), Advances in Chemical Engineering, 48, Academic Press, Cambridge MA, 2016, pp. 107–149, chapter 2.
[37] L. Liu, M.I. Mishchenko, P.W. Arnott, A study of radiative properties of fractal soot aggregates using the superposition T-matrix method, J. Quant. Spectrosc. Radiat. Transf. 109 (15) (2008) 2656–2663.
[38] L. Liu, M.I. Mishchenko, S. Menon, A. Macke, A.A. Lacis, The effect of black carbon on scattering and absorption of solar radiation by cloud droplets, J. Quant. Spectrosc. Radiat. Transf. 74 (2) (2002) 195–204.
[39] J. Charon, S. Blanco, J.-F. Cornet, J. Dauchet, M. El Hafi, R. Fournier, M.K. Abboud, S. Weitz, Monte Carlo implementation of Schiff's approximation for estimating radiative properties of homogeneous, simple-shaped and optically soft particles: application to photosynthetic micro-organisms, J. Quant. Spectrosc. Radiat. Transf. 172 (2016) 3–23.
[40] H. Li, C. Liu, L. Bi, P. Yang, G.W. Kattawar, Numerical accuracy of "equivalent" spherical approximations for computing ensemble-averaged scattering properties of fractal soot aggregates, J. Quant. Spectrosc. Radiat. Transf. 111 (14) (2010) 2127–2132.
[41] M.F. Iskander, H.Y. Chen, J.E. Penner, Optical scattering and absorption by branched chains of aerosols, Appl. Opt. 28 (15) (1989) 3083.
[42] Z.W. Cui, Y.P. Han, C.Y. Li, Characterization of the light scattering by ensembles of randomly distributed soot aggregates, J. Quant. Spectrosc. Radiat. Transf. 112 (17) (2011) 2722–2732.
[43] H. Hirose, T. Yamagishi, Illustrations of the Japanese Freshwater Algae, Uchida Rokakuho Pub, House (in Japanese), Tokyo, Japan, 1977.
[44] H. Ettl, Süßwasserflora von Mitteleuropa [Freshwater Flora of Europe], Bd. 09: Chlorophyta I: Phytomonadina 9, SpringerSpektrum, Heidelberg, Germany, 1983.
[45] T. Mizuno, E. Takahashi, An Illustrated Guide to Freshwater Zooplankton in Japan, Tokai University Press, Tokyo, Japan, 1991.
[46] M.F. Modest, Radiative Heat Transfer, 3rd edition, Academic Press, Boston, 2013.
[47] H.C. van de Hulst, Light Scattering by Small Particles, 5th edition, Dover Publications Inc, Mineola, NY, 1981.
[48] C.A. Solari, J.O. Kessler, R.E. Michod, A hydrodynamics approach to the evolution of multicellularity: flagellar motility and germ-soma differentiation in volvocalean green algae, Am. Nat. 167 (4) (2006) 537–554.
[49] J.G. Umen, Volvox and volvocine green algae, EvoDevo 11 (1) (2020) 7–15.
[50] A. Semechko, Suite of functions to perform uniform sampling of a sphere. https://github.com/AntonSemechko/S2-Sampling-Toolbox, 2012. Version 1.6.0.0.
[51] G.M. Hale, M.R. Querry, Optical constants of water in the 200-nm to 200-μm wavelength region, Appl. Opt. 12 (3) (1973) 555.
[52] M.M. Brysk, M.J. Chrispeels, Isolation of partial characterization of a hydroxyproline-rich cell wall glycoprotein and its cytoplasmic precursor, Biochim. Biophys. Acta 257 (6) (1971) 421–432.
[53] P.J. Shaw, G.J. Hills, The three-dimensional structure of the cell wall glycoprotein of Chlorogonium elongatum, J. Cell Sci. 68 (July) (1984) 271–284.
[54] D.W. Mackowski, M.I. Mishchenko, A multiple sphere T-matrix fortran code for use on parallel computer clusters, J. Quant. Spectrosc. Radiat. Transf. 112 (13) (2011) 2182–2192.
[55] D.W. Mackowski, Calculation of total cross sections of multiple-sphere clusters, J. Opt. Soc. Am. A 11 (11) (1994) 2851.
[56] D.W. Mackowski, M.I. Mishchenko, Calculation of the T matrix and the scattering matrix for ensembles of spheres, J. Opt. Soc. Am. A 13 (11) (1996) 2266.
[57] K.N. Liou, An Introduction to Atmospherica Radiation, Academic Press, San Diego, CA, 2002.
[58] L. Pottier, J. Pruvost, J. Deremetz, J.-F. Cornet, J. Legrand, C.-G. Dussap, A fully predictive model for one-dimensional light attenuation by Chlamydomonas reinhardtii in a torus photobioreactor, Biotechnol. Bioeng. 91 (2005) 569–582.
[59] R.R. Bidigare, M.E. Ondrusek, J.H. Morrow, D.A. Kiefer, In-vivo absorption properties of algal pigments, in: R.W. Spinrad (Ed.), SPIE Proceedings, Vol. 1302, Ocean Optics X, Orlando, FL, 1990, pp. 290–302.
[60] A. Souliès, J. Legrand, H. Marec, J. Pruvost, C. Castelain, T. Burghelea, J.-F. Cornet, Investigation and modeling of the effects of light spectrum and incident angle on the growth of Chlorella vulgaris in photobioreactors, Biotechnol. Prog. 32 (2) (2016) 247–261.